Reports

Observations of Solar Irradiance Variability

Abstract. *High-precision measurements of total solar irradiance, made by the active cavity radiometer irradiance monitor on the Solar Maximum Mission satellite, show the irradiance to have been variable throughout the first 153 days of observations. The corrected data resolve orbit-to-orbit variations with uncertainties as small as 0.001 percent. Irradiance fluctuations are typical of a band-limited noise spectrum with high-frequency cutoff near 0.15 day^{-1}; their amplitudes about the mean value of 1368.31 watts per square meter approach ± 0.05 percent. Two large decreases in irradiance of up to 0.2 percent lasting about 1 week are highly correlated with the development of sunspot groups. The magnitude and time scale of the irradiance variability suggest that considerable energy storage occurs within the convection zone in solar active regions.*

The active cavity radiometer irradiance monitor (ACRIM) experiment on the NASA Solar Maximum Mission (SMM) spacecraft, launched in February 1980, was designed to make regular observations of the total solar irradiance (*1*). The principle goals of the experiment are (i) to begin a climatological data base on solar irradiance variability that will cover at least one solar magnetic cycle (about 22 years) with ± 0.1 percent long-term precision, and (ii) to provide a shorter-term data base (minutes to months) with maximum precision and accuracy for the study of aspects of solar variability that are significant for solar physics investigations. This report provides a brief description of the instrument's operation and preliminary results of the first 153 days of observations.

The ACRIM instrument has three active cavity radiometer (ACR) type IV sensors, the most recent version of a series of flight pyrheliometers developed at Jet Propulsion Laboratory (*2*). Each ACR sensor is an independent, electrically self-calibrated cavity pyrheliometer, capable of defining the radiation scale at the level of total solar irradiance with precision and accuracy not previously achieved in satellite observations. The sensors view the sun through a 5° (full angle) field of view. Wavelength sensitivity is nearly uniform from the far ultraviolet through the far infrared with a cavity absorptance of 0.9995 (*3*). Separate shutters on each sensor facilitate their operation with different frequencies for all possible combinations in either automatic or manual modes. The three sensors are used in various combinations to provide periodic cross-references on the system's performance. This phased use of the three channels is designed to sustain the precision of ACRIM's observations within 0.1 percent for at least 1 year. Comparisons with other sensors on rocket and Space Shuttle payloads should sustain the multiyear precision of ACRIM within 0.1 percent for the life of the SMM. The theory and operation of ACRIM are described in (*2*).

The ACRIM observations over the first 153 days of the SMM are presented in Fig. 1. Shown are the mean values for each orbit as measured by channel A, adjusted to give the total solar irradiance at 1 A.U. and plotted as percentage variations about the mean for the 153-day period.

Each orbital mean is an integration over the solar observing portion of one orbit. It is formed by integrating 32 1-second samples from each shutter-open period and averaging the results. A maximum of 28 shutter-open solar observation periods occur per orbit. During the first 153 days of the SMM the average number of shutter-open periods per orbit was 24, corresponding to an average solar observing period of about 52 minutes during each of the 15 orbits per day. Orbital variations of ACRIM temperatures have been smaller than predicted, which enhances the resolution noise limit of the experiment. Although the irradiance data, sampled every second, have a single-sample (± 1 bit of 13) analog-to-digital uncertainty of ± 0.02 percent, the noise is sufficiently oversampled that results integrated over longer intervals show no influence from the digitization limit.

The following corrections (listed in order of significance) are applied to the irradiance measured by ACRIM: (i) normalization to a distance of 1 A.U. plus the projection of the satellite orbit on the radial direction to the sun, (ii) correction for the slow decrease in sensitivity of channel A between days 62 and 163, (iii) temperature-dependent corrections for radiation lost through the aperture and for the temperature coefficient of resistance of the cavity heating elements (*1*),

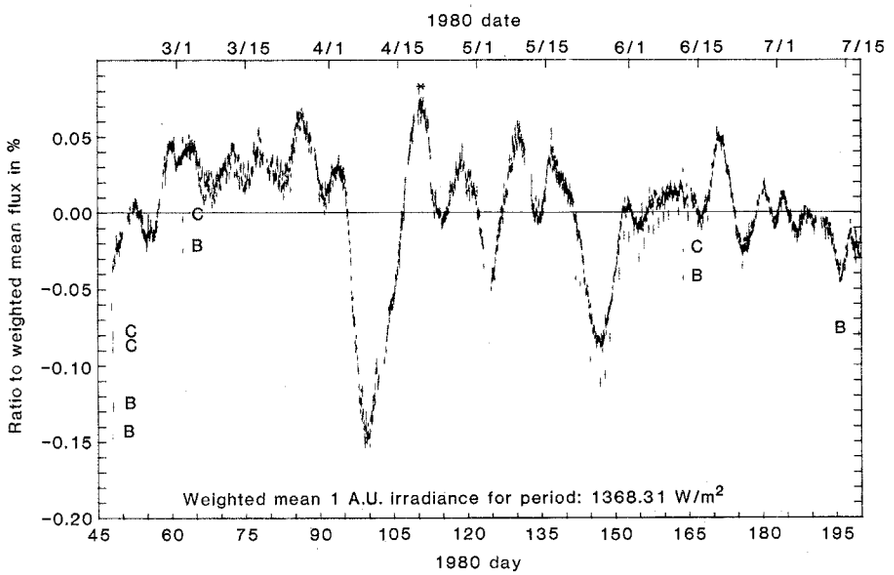

Fig. 1. Total solar irradiance at 1 A.U. for the ACRIM channel A sensor, shown as a percentage variation about the weighted mean for the first 153 days of the Solar Maximum Mission. Each tick mark represents the mean irradiance for the sunlit portion of one orbit. The horizontal extent of the tick equals the 60-minute maximum duration of the sunlit portion of an orbit. The vertical bars through the ticks are the ± 1σ standard errors of the orbital means. The ticks with associated B and C designations are the channel B and C measurements during comparisons with channel A. These results have been corrected for the small decrease in sensitivity of channel A between days 62 and 163.

0036-8075/81/0213-0700$00.75/0

(iv) correction for relativisitic radiative effects due to the relative velocity of the sun and the satellite (*4*), and (v) correction for the cosine of the angle between ACRIM's line of sight and the sun's center. These corrections are small; only the first two exceed 0.01 percent. The standard error of the relative measurements is frequently as small as 0.001 percent for one-orbit averages. There appear to be no residual atmospheric effects or sensitivity of the results to particulate fluxes (*5*).

In-flight intercomparisons of channels A, B, and C are summarized in Table 1. The only significant change in detector sensitivity was for channel A, which is used continuously to monitor the irradiance. The change between days 62 and 163 was −0.0153 percent, measured by the A/B ratio, and −0.0168 percent, measured by the A/C ratio. This drift stabilized by day 163 and no further change was detected by day 199. A slow degradation of channel A's cavity absorptance due to the effects of solar ultraviolet and particle fluxes was anticipated. Calibration by channels B and C removes its effect on ACRIM's long-term data base to within the 0.0015 percent change in the C/B ratio over the 101-day period. The irradiance record of Fig. 1 was corrected for drift in channel A, resulting in the constant relative differences shown for comparisons on days 62, 163, and 199. The larger differences between channels A, B, and C during the first few orbits on day 47 are probably due to absorption of solar flux by water vapor. Water adsorbed by the instrument before launch vaporizes in orbit at a rate dependent on the temperature of ACRIM and is released from each sensor's interior at a rate dependent on the cumulative shutter-open time for that channel.

The weighted mean value of the total solar irradiance at 1 A.U. for the first 153 days of the SMM is 1368.31 W/m², with an uncertainty in the International System of Units (SI units) of less than ± 0.5 percent. This value includes the effects of all variations observed, including the two large, temporary decreases in irradiance centered at days 99 and 146. The weighting factors used in forming the mean are the inverse squares of the standard errors of the weighted daily mean values. The latter are similarly formed from the orbital means, using their standard errors as weighting factors. These weighted means best represent the integrated irradiance for the 153-day period, with higher-precision observations having a proportionally larger influence on the overall result.

A more exact value for the "absolute" accuracy of ACRIM measurements in SI units will be determined by other experiments. The ACR type IV sensors are theoretically capable of defining the radiation scale with ± 0.1 percent uncertainty in the measurement environment of the SMM. The first principal in-flight intercomparison, conducted on day 62 after allowing 2 weeks for the spacecraft and its instruments to reach equilibrium, shows a maximum disagreement between the three independently calibrated sensors of less than ± 0.05 percent from their mean, a result consistent with the theoretical performance. Whatever the final uncertainty proves to be, the experiment is compiling a total solar irradiance record with the precision, accuracy, and time resolution required to begin a long-term climatological irradiance data base and provide quantitative new information on solar physical processes.

Table 1. In-flight intercomparisons of ACRIM sensors: ratios of irradiances measured in ACRIM channel A, B, and C sensors and their change (Δ) over the 101-day period between days 62 and 163. Channel C was not compared with A and B on day 199. The close agreement of the C/B values over 101 days is a measure of ACRIM's potential for long-term precision.

Day (1980)	A/B	ΔA/B	A/C	ΔA/C	C/B	ΔC/B
62	1.000731		1.000526		1.000205	
		−0.000153		−0.000168		0.000015
163	1.000578		1.000358		1.000219	
		0				
199	1.000578					

The most obvious features of the ACRIM observations are two large temporary decreases in irradiance in early April and late May 1980. These events, also observed by the Nimbus 7/ERB experiment (*6*), appear to be related to the behavior of specific groups of sunspots. The Zurich sunspot numbers—a conventional index of solar activity based on but not directly proportional to the area of sunspots—show small peak values around the times of these features (Fig. 2e), but this index has little significance on a radiometric scale. As an alternative to characterizing spot groups, we devised a simple method of combining measured spot areas as a predictor of the irradiance deficit due to sunspots:

$$\mathrm{PSI} = \alpha \sum \mu_i S_i \left(\frac{3\mu_i + 2}{2}\right) \qquad (1)$$

where PSI is the photometric sunspot index: α is a normalization factor; $\mu_i = \cos \theta_i$, where θ_i is the angle from our normal view of the sun; and S_i is spot area. The dependence on μ_i approximates the limb-darkening law for the quiet photosphere. Spot areas and coordinates were taken from the *Solar-Geophysical Data* issued by the National Oceanic and Atmospheric Administration. The conversion from spot area to a bolometric quantity requires an estimate of the distribution of effective temperatures within the spot. We took average values (*7*) for umbral and penumbral area fractions and temperatures, resulting in a normalization factor of $\alpha = 0.33$. Thus defined, PSI gives the estimated flux reduction in parts per million if the sunspot areas are in units of millionths of the solar hemisphere. This model, with its approximations and assumptions (*8*), can only provide a preliminary test for relations between active regions and total irradiance.

The solar irradiance and the PSI index (Fig. 2, a and b) exhibit a high degree of correlation for the 112 days of data shown—a somewhat surprising result in view of the uncertainties of the correlative data and the model approximations. The strength of the correlation derives from the strong signals observed around 8 April and 25 May (days 99 and 146). The bulk of these signals was produced by large, recently developed or devel-

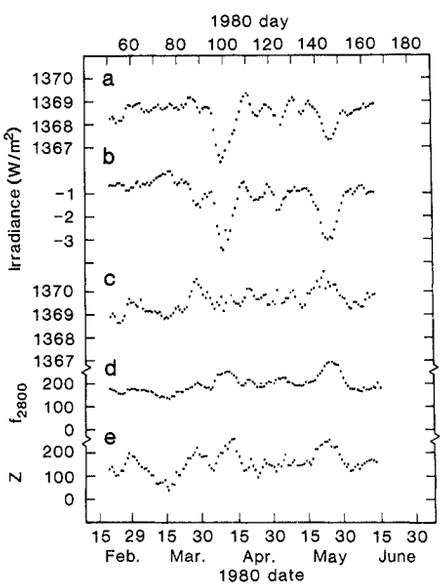

Fig. 2. Correlative plots of (a) total solar irradiance at 1 A.U., (b) photometric sunspot index (PSI), (c) irradiance adjusted by the PSI, (d) 2800-MHz index, and (e) Zurich sunspot number.

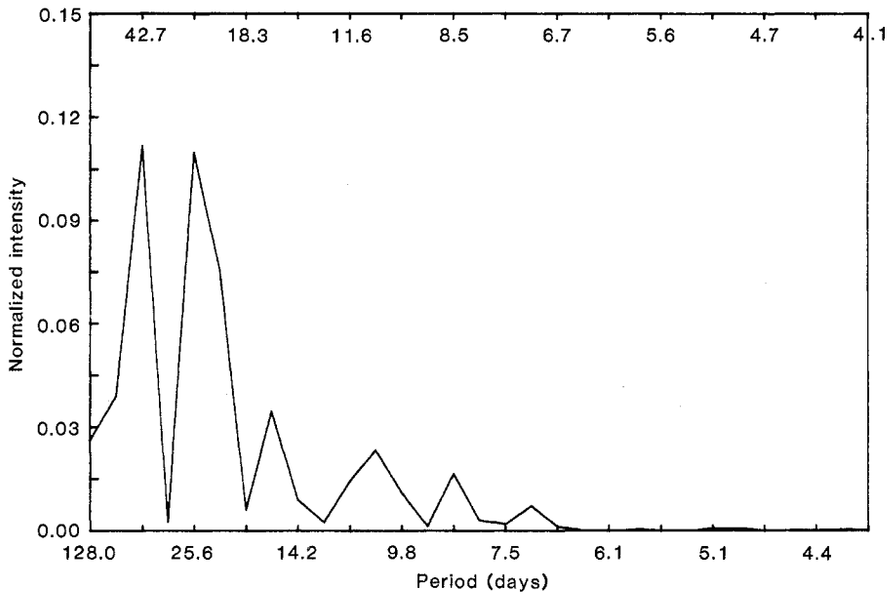

Fig. 3. Power spectrum of ACRIM daily mean irradiance record for days 52 through 179.

oping spot groups crossing the central solar meridian; on 8 April Boulder regions 2370 and 2372 on the sun contributed 80 percent of the PSI, and on 25 May regions 2469 and 2470 contributed 61 percent. These two large variations in irradiance are obviously related to the presence of such sunspot groups, and our simple PSI model satisfactorily explains not only the time profile of these events but also, in large part, their amplitudes.

Outside the times of these strong signals, the correlation between spot index and solar irradiance is not as good, and significant deviations from the pattern exist. The first 35 days of data give no indication of a correlation. Furthermore, there is a difference in detail between the two major dips in irradiance described above. The difference signal (Fig. 2c) shows no trace of the dip in early April, but shows a large positive excursion at the time of the May dip, presumably the effect of the larger facular component observed to be associated with the latter.

Finally, a 5-day drop in solar irradiance centered on 13 May (day 134) seems to have no counterpart in solar activity of the type discussed above. The presence of such short-term variations of irradiance, uncorrelated with obvious solar activity processes, suggests other sources of solar variability. The list of possible sources is a long one (*5*, *9–12*) and their identification has just begun.

The other major obvious contributor to the total solar irradiance is the aggregate of white-light faculae. We would expect the difference between the irradiance (Fig. 2a) and the sunspot effect estimated by PSI (Fig. 2b) to show a good correlation with some measure of these regions of excess solar emission. The 2800-MHz index (Fig. 2d), a reliable indicator of emission activity, does not show a high correlation with the adjusted irradiance (Fig. 2c) for the entire data set. Identification of facular contributions to solar irradiance will require more precise independent measures of facular brightness than are now available (*13*).

The apparent relation between the evolution of large sunspot groups and the two large irradiance events in April and May has a bearing on the nature of convective energy flow in solar active regions. We conclude that, at least in these two cases, there is no direct and immediate energy balance between sunspot deficit and facular excess; instead, the sunspot-deficit energy is stored or delayed within the convection zone through the effects of the magnetic fields associated with the sunspot groups involved (*14*). Subsequent development of related faculae in these regions may provide the mechanism for radiating the stored energy away. Further study of these and similar events should provide interesting information about the deep structure of active regions.

The continuous variability of the ACRIM irradiance record with smaller amplitudes than those of the big dips is another interesting feature. Preliminary time series analyses have been performed on the daily mean values to investigate this variability. The power spectrum of the irradiance at 1 A.U. for days 52 through 179 is shown in Fig. 3. We assign little significance to the individual spectral peaks, since their periods are large compared with the length of the data base and the two big dips, which we assume to be aperiodic, undoubtedly distort the spectrum. The most interesting feature is the cutoff of spectral intensity for periods shorter than about 7 days.

A second time series analysis was performed on the PSI-adjusted flux to eliminate most of the effects of the two big dips. The result showed essentially the same spectrum (but with lower relative significance for the spectral peaks) with the 7-day cutoff.

The results of these analyses are typical of a band-limited noise spectrum. The one significant feature at this point is the cutoff of spectral power density at about 7 days. This result is consistent with the emergence and development of sunspot groups and associated facular areas, occurring at apparently unrelated intervals and locations, which take on the order of 7 days or more to complete their evolution.

R. C. WILLSON
S. GULKIS, M. JANSSEN
Jet Propulsion Laboratory, California Institute of Technology, Pasadena 91103

H. S. HUDSON
Center for Astrophysics and Space Sciences, University of California, San Diego 92093

G. A. CHAPMAN
San Fernando Observatory, California State University, Northridge 91330

References and Notes

1. The SMM spacecraft is in a circular orbit at 575 km with a 28.5° inclination. During the orbital period of 96 minutes, the spacecraft spends about 60 minutes in full view of the sun.
2. R. C. Willson, *Appl. Opt.* **18**, 179 (1979).
3. E. Zalewski, J. Geist, R. C. Willson, *Proc. Soc. Phot.-Opt. Instrum. Eng.* **196**, 152 (1979).
4. R. C. Willson and H. S. Hudson, paper presented at the COSPAR (Committee on Space Research) meeting, Budapest, June 1980.
5. _____, *Astrophys. J. Lett.*, in press.
6. J. R. Hickey, personal communication.
7. C. W. Allen, *Astrophysical Quantities* (Athlone, London, 1973).
8. Spot groups differ in properties and can be described only approximately by average values. The behavior of small spots may be quite different from that of the large ones that dominate the signal. The PSI values do not include any estimate of facular excess emission.
9. P. V. Foukal and J. E. Vernazza, *Astrophys. J. Lett.* **234**, 707 (1979).
10. R. K. Ulrich, *Science* **190**, 619 (1975).
11. D. O. Gough, in *The Solar Output and Its Variations*, O. R. White, Ed. (Colorado Associated Univ. Press, Boulder, 1977), p. 95.
12. R. H. Dicke, *Nature (London)* **276**, 676 (1978).
13. G. A. Chapman, *Astrophys. J. Lett.*, in press.
14. For this conclusion to be at variance with the observations there would have to be either rapid redistribution of the deficit energy to distant regions of the sun less visible or invisible to ACRIM or conversion to other forms of energy not detectable by ACRIM.
15. We thank R. Noble and M. Woodward for their valuable assistance in data processing and interpretation. The SMM/ACRIM experiment is supported by NASA grants NAS-7-100 at Jet Propulsion Laboratory, NSG-5322 at the University of California at San Diego, and NSG-5330 at the California State University, Northridge, Foundation.

18 September 1980; revised 24 November 1980